Calibrating and Comparing Autonomous Braking Systems in Motorized-to-Non-Motorized-Vehicle Conflict Scenarios

Weixuan Zhou and Xuesong Wang

***Abstract*— Assuring the safety of all road users, including non-motorized vehicles, is important in the autonomous driving environment. Autonomous emergency braking (AEB) systems have provided an effective way for automated vehicles to avoid collisions with the less easily detectable non-motorized vehicles. Automatic preventive braking (APB) is a new method proposed by Mobileye that promises to reduce crashes without reducing traffic throughput, but APB's effectiveness has not yet been evaluated. This study therefore calibrates and compares the performance of APB with that of one-stage and three-stage AEB braking systems in safety-critical events (SCEs) between motorized and non-motorized vehicles, using SCEs extracted from the Shanghai Naturalistic Driving Study and simulated in MATLAB's Simulink. The evaluation results, which consider both safety and conservativeness, show that 1) one-stage AEB with a deceleration of 5.5 m/s^2 and a time-to-collision threshold of 1.6 seconds can prevent all SCEs from becoming crashes; 2) APB has the best driving stability but its safety performance is inferior to that of the two AEB systems; 3) APB's deceleration process is easily affected by its pre-defined parameters and changing kinetic parameters, which may be one cause of its crashes; 4) AEB's time-triggered braking process is more consistent and reliable than APB's distance-triggered process.**

***Index Terms*— Automatic preventive braking, autonomous emergency braking, motorized-to-non-motorized-vehicle-conflict, safety-critical event.**

I. Introduction

AUTOMATED vehicles, at both partial and high levels of automation, have achieved outstanding performance in controlled environments. Variously known as autonomous and ego vehicles, automated vehicles (AVs; see Appendix TABLE 8 for all abbreviations) will eventually be traveling in much more complex environments, with multiple road users including pedestrians and non-motorized vehicles (NMVs). NMVs such as bicycles and e-bikes (often but not always considered as NMVs), with their various appearances and flexible trajectories, create challenges for the AV's detection, intention prediction, and motion planning systems [1], [2]. In China, bicycles and e-bikes are widely used for commuting and delivering goods. It is estimated that China has the largest number of NMVs in the world (nearly 400 million bicycles and 300 million e-bikes) [3], and they have a high accident rate. In 2015 alone, NMV-related crashes were overrepresented as 63.9% and 82.3% of fatal and injury crashes, respectively, in Shanghai [4]. The proportion of fatal crashes involving powered two-wheelers, or e-bikes, is also high (60% - 70%), not only in China but in other Asian countries such as Thailand, Cambodia, and Indonesia [5]. Europe, too, is starting to experience increasing fatality rates for e-bikes. For example, Sweden had a 10% increase in powered two-wheeler road fatalities from 2000 to 2018, a period in which the total number of road fatalities decreased significantly [6]. With the current rapid development of automated vehicles and the challenges NMVs pose to them, the NMV road safety issue will persist. It is crucial to explore ways to assure the safety of the non-motorized vehicle in the autonomous driving environment.

The autonomous emergency braking (AEB) system, an essential function of advanced driving assistant systems (ADAS), has been shown to considerably reduce traffic accidents [7], [8]. To adapt AEB to the characteristics of cyclists, an AEB cyclist system was developed by SafetyCube DSS, the European Road Safety Decision Support System, and is currently on the market [9]. To evaluate the cyclist braking system on equipped vehicles (that are not test vehicles), the European New Car Assessment Programme (EuroNCAP) developed a test system and protocol based on car-to-cyclist scenarios, the system and protocol of which have been implemented in consumer rating tests [10]. Studies have shown that AEB systems are effective in mitigating rear-end crashes between passenger cars and NMVs [11], [12], and have great potential benefit if widely applied [13]. The activation condition and collision avoidance patterns, however, differ among systems. AEB activation is variously based on time-related conditions, or triggers, such as time-to-collision (TTC), and distance-related triggers, such as safety braking distance [14], [15]. Collision avoidance patterns in cars currently on the road consist of multiple braking stages such as warning, brake support, and partial and full automatic emergency braking [16]. Researchers have conducted simulation and field tests of braking systems with different combinations of braking stages, however,

Manuscript received 28 May 2021; revised 28 January 2022; accepted 22 April 2022. Date of publication 4 May 2022; date of current version 7 November 2022. This work was supported in part by the Chinese National Science Foundation under Grant 51878498, in part by the European Commission H2020 Project LEVITATE (Societal level impacts of connected and automated vehicles) under Grant 824361, and in part by the Intel Corporate under the project of Evaluation of Roadway Infrastructures Readiness for Autonomous Vehicles. The Associate Editor for this article was J. Alvarez. *(Corresponding author: Xuesong Wang.)*

The authors are with the College of Transportation Engineering, Tongji University, Jiading, Shanghai 201804, China (e-mail: 1651404@tongji.edu.cn; wangxs@tongji.edu.cn).

Digital Object Identifier 10.1109/TITS.2022.3170978

few studies have taken into consideration both activation condition and collision avoidance pattern.

Automatic preventive braking (APB), like AEB, is a collision avoidance system that aims to reduce crashes, but it also aims to do so without compromising traffic flow and driving comfort by applying a mild brake and at an early stage [17]. APB is part of the ADAS that incorporates Responsibility-Sensitive Safety (RSS) into autonomous braking system. RSS is a formal model, that is, if all vehicles were to follow the rules on which the model is based, theoretically, no crashes would occur; the RSS model has been demonstrated to provide safety assurance in safety-critical car-following and cut-in scenarios [18], [19]. APB employs a distance-related trigger and is designed to prevent the vehicle from getting into unsafe situations by using safe distance as the key criterion. APB's jerk-bounded braking profile and idea of safe distance is very thought provoking, and has aroused the interest of many researchers [20], [21], but few studies have evaluated the effectiveness of APB or calibrated its parameters with real driving data, especially conflicts with non-motorized vehicles. As it is essential to validate the real effectiveness of any newly proposed method as well as to discover its potential application and potential problems, the main objective of this study is therefore to determine the relative advantages to motorized-to-non-motorized vehicle safety of the APB and AEB systems.

Traffic research typically uses crash data to determine safety. For example, previous studies of AEB have used in-depth accident data to recreate pre-crash scenarios to estimate AEB's benefit in terms of number of collisions mitigated or eliminated [22], [23]. However, crashes are rare events, which makes it infeasible to collect an adequate quantity of crash data in a limited study period [24]. Drivers are more likely to encounter safety-critical events (SCEs), scenarios that are likely to cause a crash if avoidance maneuvers are not taken in time. An autonomous braking system such as AEB or APB should, in theory, help to defuse the risk of SCEs becoming crashes, but the benefit of braking systems in preventing SCEs from deteriorating into crashes has not been tested. Another reason to use the SCE for testing autonomous braking systems is that it is a less severe traffic conflict than the crash, so there is reason to expect that the AEB maneuvers used to evade crashes may be too aggressive for the SCE. The strong brake pressure applied by the AEB (usually up to 1.0 g) may not be necessary for the less severe and more common SCE, and because an overly conservative system with excessive braking can lead to frequent false alarms and disturb the driver, a less conservative braking approach may be warranted. Therefore, in addition to comparing the AEB and APB systems, a primary purpose of this study is to calibrate the parameters of the braking process to be suitable for the SCE; in particular, the proper deceleration rate, jerk, and brake activation time for the SCE should be determined.

SCE data can be readily collected by naturalistic driving studies (NDS), in which instrumented vehicles collect driving data from large numbers of drivers over a period of time [25]. The NDS reflects the real unsafe situations drivers encounter daily, so offer sufficient data to rebuild the scenarios for study. This study uses motorized-to-non-motorized-vehicle SCEs from the Shanghai Naturalistic Driving Study (SH-NDS) to calibrate and evaluate three autonomous braking systems: APB, one-stage AEB, and three-stage AEB, the latter two of which are representative of the commonly used AEB systems. Non-motorized vehicles are specifically defined in this study to include bicycles and e-bikes, but to exclude motorcycles. The procedures of the study are as follows: 1) extract motorized-to-non-motorized vehicle SCEs using a trigger method combined with manual validation; 2) rebuild the SCEs in the MATLAB simulation platform and control the subject ego vehicle with each of the three braking systems; 3) calibrate all the systems by testing their driving safety and conservativeness under different parameter combinations; 4) compare their performance in safety and conservativeness; and 5) explore the underlying reasons for crashes in order to improve the autonomous braking systems in future research and development.

II. Literature Review

A. Safety-Critical Events (SCEs)

In the 100-Car naturalistic driving study, the first of its kind, the events were classified according to their severity as crash, near-crash, crash-relevant conflict, and proximity conflict. Near-crashes involve circumstances that require rapid evasive maneuvers by the subject vehicle, or any other vehicle, pedestrian, cyclist, or animal to avoid a crash. In crash-relevant conflicts, the evasive maneuvers are less severe [26]. Previous studies have found that a positive relationship exists between crashes and near-crashes [27], and that the number of near-crashes can be used to predict crash frequency by both logit and probit models [28]. Guo *et al.* [29] found that the rate of critical incidents, their term for crash-relevant conflicts, had significant impact on crash and near-crash risk. The causal mechanisms of crashes, near-crashes and critical incidents have thus been demonstrated as similar, the major differences between them being the severity of the events as well as the activation time and intensity of the evasive maneuvers.

B. Autonomous Emergency Braking (AEB)

AEB systems that have been tested and are available to the consumer can be classified into at least three categories: 1) one-stage AEB activated by a time-related trigger such as TTC or a distance-related trigger such as safe braking distance, 2) AEB combined with forward collision warning (FCW), and 3) multi-stage AEB with or without FCW [30]–[32]. The most fundamental and commonly used collision avoidance pattern is one-stage AEB activated by TTC [33]. In this AEB system, when the TTC drops below a pre-defined value (usually between 0.5 s and 1.5 s), the vehicle automatically performs an emergency braking maneuver. Some manufactures such as Audi, Volvo, and Volkswagen combine FCW with partial and full autonomous braking together into multi-stage systems. The intent of these combined systems is to best assist drivers by giving them enough time to perform a proper evasive maneuver, and then provide full brake when a crash becomes otherwise unavoidable [30]. The three-stage AEB used in the Audi A7 has been tested and shown to perform

well [30], as has the basic and commonly used one-stage AEB [10], [11]. This study will therefore compare the performance of these two AEB systems with the APB in safety-critical events between motorized and non-motorized vehicles.

Previous studies have used different methods to calibrate the parameters of AEB systems. Rosén [11] investigated the performance of a one-stage AEB by varying the values of TTC, deceleration, and other relevant parameters. Results showed a TTC of 1.5 s and a max deceleration of 0.9 g were optimum. Zhao *et al.* [34] found optimal TTC combinations for a two-stage AEB by listing the TTC values in typical control strategies, and identifying reasonable combinations by constraining the time interval between the two TTC values. A two-stage AEB with TTC = 1.0 s at the first stage and TTC = 0.6 s at the second stage were optimum. Peng *et al.* [35] determined the best AEB parameter values by solving a multi-objective optimization problem using the NSGA-II algorithm. A TTC of 1.737 s with a deceleration of 7.428 m/s^2 and a sensor detection angle of 180° were optimum.

C. Automatic Preventive Braking (APB)

The automatic preventive braking (APB) system is a collision avoidance system that originally defined a braking profile similar to the way that RSS [36] responds, which is for the equipped following vehicle to decelerate with at least the minimum reasonable brake value when the relative distance to the lead vehicle is shorter than safe distance. To make the braking mild and thus comfortable, APB redefined the longitudinal safe distance by substituting the following vehicle's braking profile with a jerk-bounded profile. Instead of braking at a constant deceleration, the following vehicle decelerates linearly, from its current acceleration, at a constant rate of change in acceleration, or jerk, until it reaches a level of braking that will allow it to create a safe distance or to stop before colliding with the lead vehicle. The following vehicle continues to brake at this minimum reasonable brake until it stops or the distance becomes safe [17].

Mattas *et al.* [37] have tested APB's performance in rear-end collisions. The results of their experiment showed that including jerk in the calculation of safe distance makes the approach more accurate than other braking approaches that do not consider it. The researchers also discovered that the subject ego vehicle's maximum decelerations of 3 m/s^2 and 9 m/s^2 were, respectively, either too smooth or too aggressive, and that the values between them may achieve a better tradeoff between decelerating too hard or too often. However, no studies have focused on calibrating and evaluating the APB system for motorized-to-non-motorized-vehicle conflict events. One of the current study's aims is therefore to validate the real effectiveness of APB in these events and to discover its applicable situations and any underlying problems.

III. Data Preparation

A. Extraction of Safety-Critical Events

The Shanghai Naturalistic Driving Study (SH-NDS) was the first naturalistic driving study in China. The data collection effort was conducted collaboratively by Tongji University, General Motors, and the Virginia Tech Transportation Institute. Five test cars were equipped with advanced data acquisition systems [38] that included four cameras (facing front, rear, driver's hands, and driver's face), radar, GPS, speedometer, three-dimensional accelerometer, and the Mobileye C2-270 collision prevention system [39]. The three-year data collection started in December 2012 and ended in December 2015. A total of 19,133 trips with 161,055 driven kilometers were recorded.

Safety-critical events (SCEs) are most commonly extracted from NDS data based on the evasive maneuvers used to avoid a crash: steering, braking, accelerating, or any combination of these maneuvers. The SCEs are extracted in a two-step process: 1) automatically filtering the kinematic parameters (longitudinal/lateral deceleration, yaw rate, and TTC) by setting a group of trigger criteria, and 2) manually validating each automatically extracted event by watching the front-view video of the instrumented vehicle involved in the event.

The SCEs in this study included near-crash and crash-relevant conflicts between cars and NMVs, which are defined in this study to include bicycles and e-bikes, but to exclude motorcycles. With the SH-NDS's rich kinematic and video data obtained from real-life driving, the SCEs for this study could be extracted. In the first extraction step the kinematic data were automatically filtered by a series of criteria to extract the candidate events with high longitudinal and lateral acceleration and low TTC. In the second step, the events were manually viewed to eliminate other types of events such as car-to-car, car-to-motorcycle and car-to-pedestrian conflicts.

The extraction trigger criteria were initially set in accord with the 100-car Naturalistic Driving Study [26] and the second Strategic Highway Research Program (SHRP2) [40], and adjusted based on the specific characteristics of motorized-to-non-motorized vehicle events [39]. Further detail on trigger criteria is available in existing literature [18]. The criteria for this study were as follows:

Trigger 1: Longitudinal acceleration less than or equal to −0.6 g;

Trigger 2: Lateral acceleration greater than or equal to 0.75 g, or less than or equal to −0.75 g;

Trigger 3: Manual activation by the driver pressing a button on the dashboard when an event occurred that he/she deemed critical;

Trigger 4: Longitudinal acceleration less than or equal to −0.5 g coupled with forward TTC less than or equal to 4 s;

Trigger 5: Longitudinal acceleration less than or equal to −0.4 g coupled with forward TTC less than or equal to 4 s and relative distance to the non-motorized vehicle less than or equal to 30 m.

After manually validating the filtered videos, 136 SCEs were extracted, and then were categorized by the scenarios introduced in EuroNCAP's cyclist-AEB testing system (CATS) [10]. Four basic categories were defined by the maneuver of the motorized vehicle and the relative orientation of the NMV with respect to the vehicle, they are: crossing (C), longitudinal (L), on-coming (On) and turning (T). The four categories were further divided into 12 scenarios based on the maneuver of the NMV. The few remaining events were

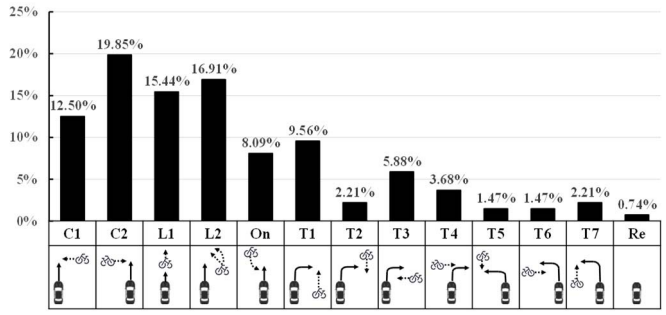

Fig. 1. Types and distribution of safety-critical events.

classified as remaining (Re). The most commonly occurring scenarios in this study were longitudinal and crossing scenarios, which accounted for 32.35% (L1+L2) and 32.35% (C1+C2) of all extracted events (Fig. 1). The majority of crossing and turning conflicts happened at intersections, while most longitudinal conflicts happened on non-intersection road segments. The proportion of crossing scenarios was quite close to the 35.87% collected in another study from naturalistic driving data in Beijing [42], but the proportion of longitudinal scenarios was significantly higher in Shanghai than in Beijing (19.57%). The majority of longitudinal events in Shanghai occurred on 1) single lane streets, 2) roads without bicycle lanes, and 3) roads where bicycle lanes were occupied by parked cars. Illegal parking and lack of bicycle lanes are common conditions in Shanghai, which may lead to frequent conflicts between motorized and non-motorized vehicles. To provide a base for future research to seek a solution to this problem, this study's analysis focused on the longitudinal conflict events.

Due to radar detection limitations, it was suspected that the non-motorized vehicles in some of the events were not detected and were therefore omitted as TTC could not be calculated. To find events such as these that may have been omitted, all the trips were filtered again by using the Mobileye pedestrian and cyclist warning (PCW) system as a trigger. This trigger extracted 316 additional events, but as the PCW trigger criteria are less strict than the criteria otherwise used in this study, many were deemed less critical after carefully reevaluating and validating the videos and data. In the end, a total of 108 longitudinal conflict events with data adequate to rebuild the scenarios were used in this study. The longitudinal acceleration was less than -0.4 g for 41 of these conflicts, and was greater than -0.4 g for the remaining 67.

B. Analysis of the Extracted Events

The main parameters of one-stage AEB are the TTC (TTC_b) and deceleration (d_{one}) thresholds; for three-stage AEB, the parameters are the three deceleration values (d^1_{three}, d^2_{three} and d^3_{three}); and for APB they are the minimum reasonable brake of the subject ego vehicle ($a_{min,brake}$), maximum jerk of the ego vehicle (j_{max}), and maximum possible brake of the non-motorized vehicle ($a_{max,brake}$). While the AEB parameters are self-explanatory, the APB parameters, particularly the maximum deceleration of the subject ego vehicle ($a_{min,brake}$), warrant illustration. In a typical SCE, the NMV is the lead vehicle, so its maximum brake influences the response of the following APB-equipped subject vehicle. The subject vehicle will not collide with the NMV as long as it brakes with a constant jerk until it reaches the minimum reasonable brake. The minimum brake is designed to ensure the gentlest possible braking while remaining safe.

TABLE I

50th, 75th, 95th PERCENTILE OF SUBJ VEH MIN REASONABLE DECEL, SUBJ VEH MAX JERK, NMV MAX DECEL, AND SUBJ VEH INITIAL VELOCITY

Percentile	Subj veh min reasonable decel (m/s^2)	Subj veh max jerk (g)	NMV max decel (m/s^2)	Subj veh initial velocity (m/s)
50%	2.60	0.74	2.05	8.89
75%	4.33	1.10	3.33	11.27
95%	5.59	2.34	5.83	16.36

The distributions of these and additional important parameters of the 108 longitudinal motorized-to-non-motorized vehicle events are shown in the histograms in Fig. 2, where the cumulative distributions are indicated by the red lines. The event duration should logically cover the entire length of the conflict; however, due to occlusion and the detection limitations noted above, many of the NMVs were detected only when they were very close to the subject vehicle, with the consequence that the event duration varies greatly in Fig. 2(a). Most of the events are quite urgent: as is shown in Fig. 2(c), the minimum TTC in 60% of the events is lower than 1 s. The decelerations shown in Fig. 2(e) and 2(g) are the absolute values of the acceleration. The decelerations indicated in the rest of the paper will follow the same rule of being absolute values.

The braking systems to be compared, that is, the one-stage AEB, three-stage AEB, and APB systems, are designed in this study to handle safety-critical events, not crashes. Therefore the threshold values of the parameters in the three models should not be as critical as the values designed to prevent crashes. To ensure that the parameters can best represent actual driving conditions and cover most of the scenarios in the extracted events, the values that will be used in Section IV will refer to the 50th, 75th, and 95th percentiles of the four critical parameters shown in TABLE I.

C. Safety-Critical Scenario Generation

To rebuild the SCEs into scenarios in the simulator, the velocity and trajectory of the non-motorized vehicles (NMVs) were generated from the kinetic parameters recorded by the subject vehicles and extracted from the naturalistic driving study (NDS) data. These kinetic parameters were the velocity of the subject vehicle, and the relative distance and relative velocity of the subject vehicle and the NMV.

As is shown in Fig. 3, the simulation generating process can be divided into two steps. In step 1, the longitudinal and lateral

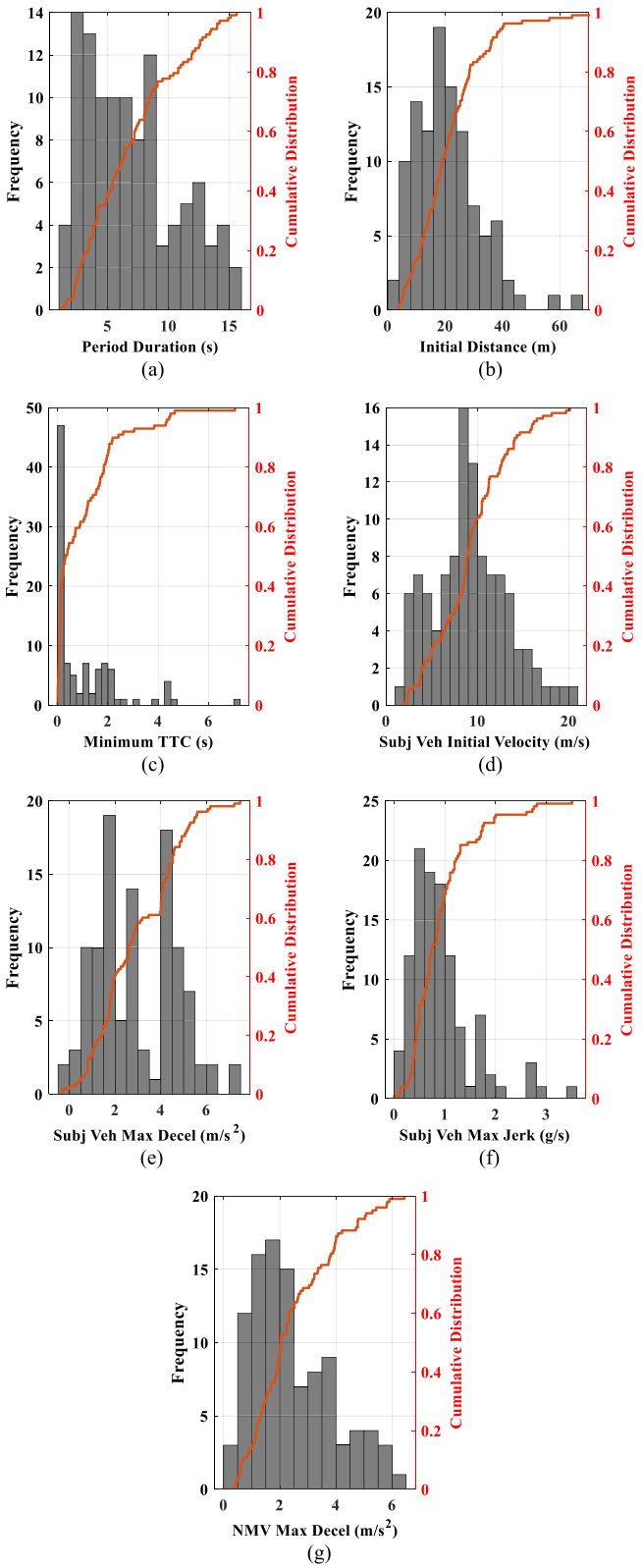

Fig. 2. Distributions of event duration; initial distance; minimum TTC; subject vehicle's initial velocity, maximum deceleration, and maximum jerk; and NMV's maximum deceleration.

velocity of the NMV at each simulation step i was derived from the subject vehicle's velocity and the relative velocity between the vehicles. In step 2, the trajectory of the NMV

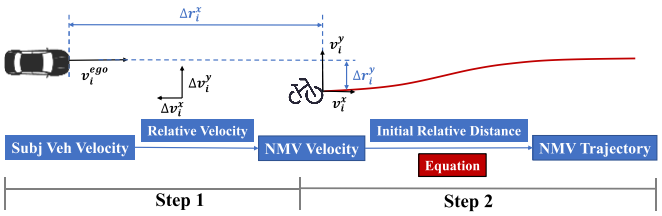

Fig. 3. Generating the velocity and trajectory of the non-motorized vehicle.

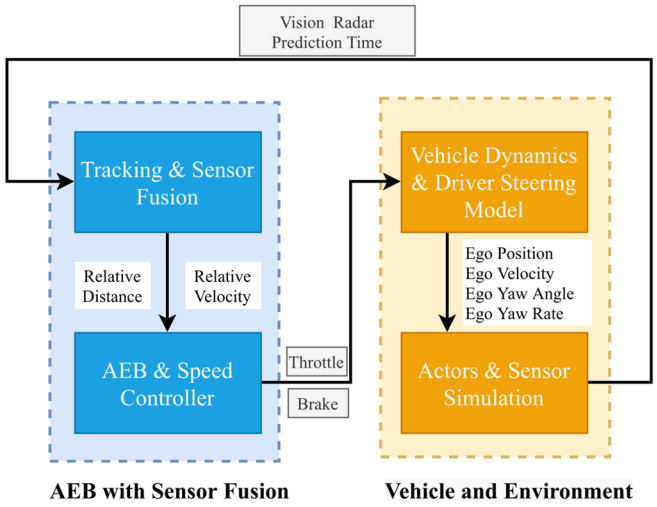

Fig. 4. Simulation procedure of AEB in simulink.

was derived from its own velocity by the following equation:

$$P_i^x = \begin{cases} P_{i-1}^x + v_i^x \times \Delta t, & i \geq 2 \\ \Delta r_1^x, & i = 1 \end{cases}$$
$$P_i^y = \begin{cases} P_{i-1}^y + v_i^y \times \Delta t, & i \geq 2 \\ \Delta r_1^y, & i = 1 \end{cases} \quad (1)$$

where P_i^x and P_i^y denote the longitudinal and lateral position of the NMV, respectively; v_i^x and v_i^y denote the NMV's longitudinal and lateral velocity; Δt denotes the simulation step length, which is 0.1 s in this study; and Δr_1^x and Δr_1^y are the initial relative distances between the two vehicles. The initial position of the subject vehicle was set as (0,0) in the simulation, so the initial position of the NMV should be the initial relative distance between the two vehicles.

IV. Methodology

A. Simulation Platform

This study used the MATLAB Automatic Driving Toolbox to create and virtualize the driving scenarios and to simulate driving behavior under the controlling algorithms. The simulation was realized by the collaboration of two subsystems consisting of four blocks. Fig. 4 illustrates the blocks designed in Simulink to test the AEB system. The APB system uses the same simulation structure, simply replacing the AEB controller with the APB controller.

In the *AEB with sensor fusion* subsystem shown on the left, the *tracking and sensor fusion* block fuses the data from the

TABLE II
SUMMARY OF THE 5 ONE-STAGE AEB ALGORITHMS UNDER STUDY

	d_{one} (m/s^2)	Ego Initial Velocity (m/s)	TTC_b (s)
1-stage AEB 1	4.5	9.0	2.0
1-stage AEB 2	4.5	11.0	2.4
1-stage AEB 3	5.5	9.0	1.6
1-stage AEB 4	5.5	11.0	2.0
1-stage AEB 5	5.5	16.5	3.0

sensors and detects the most important object (MIO), as well as its position and velocity. The *AEB and speed controller* block decides the driving strategy of the next simulation step by analyzing the current safety condition, and outputs the brake pressure or throttle to the *vehicle and environment* subsystem. The *vehicle dynamics and driver steering model* block models the dynamics of the simulated subject vehicle, now the ego car, as it drives along the road's various alignments. The motion of the ego car is synchronized in the scenario by the *actors and sensor simulation* block, after which the sensors output the data for the next step in the simulation.

B. One-Stage AEB System

The one-stage autonomous emergency braking system modeled in this study was chosen for comparison because it is simple and widely used. It is the basic AEB, in which the vehicle brakes with a constant deceleration d_{one} when the TTC is shorter than the threshold TTC_b (Fig. 5). The algorithm depends on these two pre-defined parameters, deceleration and TTC, and does not apply any speed dependent parameters.

In the one-stage AEB simulation, the ego car is designed to drive at its initial velocity until it brakes with d_{one}, so the time that the ego car requires to achieve a full brake is its initial velocity divided by d_{one}, namely TTC_b. The values used for d_{one} and initial velocity are approximations of the 50th, 75th, and 95th percentiles of the subject vehicle's maximum deceleration and initial velocity parameters in TABLE I. Nine one-stage AEB algorithms were initially generated: 3 ×3 combinations of deceleration and TTC threshold values. Four algorithms with TTC_b larger than 3.0 s were removed to ensure that the system was not activated too early. A total of five one-stage AEB algorithms were thus studied (TABLE II).

C. Three-Stage AEB System

The second system chosen for comparison was a three-stage cascaded AEB with early forward collision warning (FCW). The system is similar to the Audi A7's emergency braking system, which was demonstrated to have good performance by the Allgemeiner Deutscher Automobil-Club (ADAC) comparative test of advanced emergency braking systems [30]. In this three-stage AEB system, the initial action comes from the FCW, but the FCW's activation depends on a stopping time calculation, a parameter that varies with the speed, in this case, of the ego car. Stopping time, which refers to the period from when the ego car first applies its brake a_{brake} to the time it comes to a complete stop, is continuously compared with the current TTC. Eq. 2 is the general equation for stopping time. When

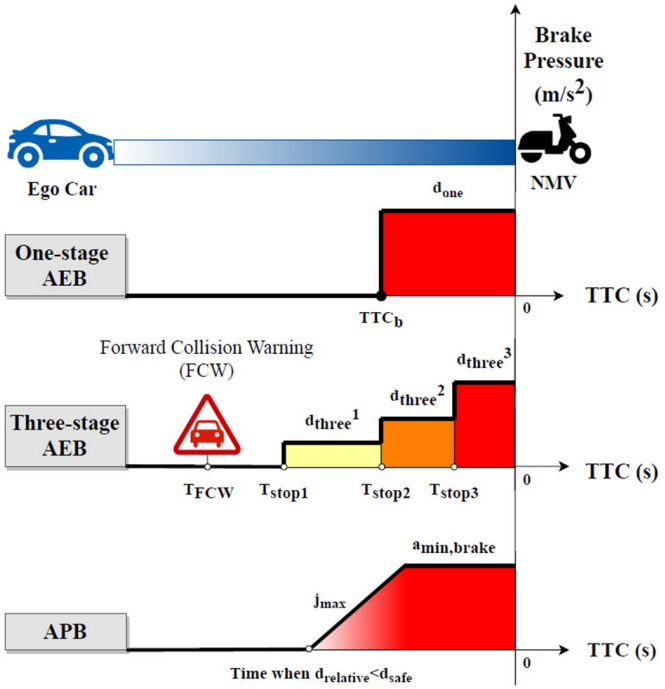

Fig. 5. Braking profiles of one-stage AEB, three-stage AEB and APB models.

calculating FCW stopping time (τ_{FCW}), this a_{brake} variable is renamed as a_{driver} in Eq. 3 to differentiate it from a_{brake}after AEB is activated, in which a_{brake} will be d^1_{three}, d^2_{three} and d^3_{three} for each of the three stages.

$$\tau_{stop} = \frac{v_{ego}}{a_{brake}} \tag{2}$$

When the FCW system alerts the driver to an imminent collision, the driver is expected to apply the brake (a_{driver}) after a reaction time τ_{react}, making the total ego car stopping time τ_{FCW}:

$$\tau_{FCW} = \tau_{react} + \tau_{stop} = \tau_{react} + v_{ego}/a_{driver} \tag{3}$$

As is shown in Fig. 5, if TTC is shorter than τ_{FCW}, the FCW is activated. If the driver fails to apply the brake in time, the AEB is activated. The three stages of this system refer to three levels of brake pressure, which, in this study, correspond to the percentiles of the subject vehicle's maximum deceleration (TABLE I). The brake pressure of the first stage is at the 50th percentile ($d^1_{three} = 2.5\,m/s^2$), at the second stage pressure is at the 75th percentile ($d^2_{three} = 4.5\,m/s^2$), and third stage full brake is at the 95th percentile ($d^3_{three} = 5.5\,m/s^2$). The stopping time at each braking stage is calculated with Eq. 2, and if the TTC is shorter than the stopping time at that stage, brake pressure is applied.

Whereas one-stage AEB has five algorithms due to its five combinations of parameter values, three-stage AEB has only one combination because the system employs all three percentiles.

D. APB System

As mentioned earlier, the decision making and control procedures of the automatic preventative braking (APB)

algorithm, having originated in the RSS model, are similar to those of the RSS: in a car-following situation, the following vehicle continuously compares its relative distance to the lead vehicle with the safe distance, which is the difference in distance that each of the two vehicles require to reach a full stop. When the car enters an unsafe driving condition it will decelerate until it stops or the distance becomes safe. To make the braking gentler, APB redefined the longitudinal safe distance between the lead and following vehicles by substituting the original braking profile of the following vehicle with a jerk-bounded profile (Fig. 5). That is, instead of braking with a minimum reasonable braking value $a_{min,brake}$, the vehicle brakes with a constant rate of change in acceleration, or constant jerk j_{max}, until it reaches the $a_{min,brake}$. The simulated ego car's jerk-bounded braking profile is as follows:

$$a(t) = \begin{cases} a_0 - j_{\max} t, & a(t) > -a_{\min,brake} \\ -a_{\min,brake}, & else \end{cases} \tag{4}$$

It is assumed that the vehicle can reach zero acceleration immediately, so its initial acceleration is set as $a_0 \leq 0$.

Based on the jerk-bounded profile, the braking distance is defined as follows:

$$\begin{aligned} d_{brake} = & [v_0 T + \frac{1}{2} a_0 T^2 - \frac{1}{6} j_{\max} T^3] \\ & + \frac{(v_0 + a_0 T - \frac{1}{2} j_{\max} T^2)^2}{2 a_{\min,brake}} \end{aligned} \tag{5}$$

where T is the first time in which either $a(T) = -a_{min,brake}$ or $v(t) = 0$; that is,

$$\begin{aligned} T_1 &= \frac{a_0 + a_{\min,brake}}{j_{\max}} \\ T_2 &= \frac{a_0 + \sqrt{a_0^2 + 2 j_{\max} v_0}}{j_{\max}} \\ T &= \min\{T_1, T_2\} \end{aligned} \tag{6}$$

The lead vehicle (NMV in this study) travels at speed v_f and decelerates, at the most, at $a_{max,brake}$; thus, the safe distance formula:

$$d_{safe} = \left[\begin{array}{l} \left[v_0 T + \frac{1}{2} a_0 T^2 - \frac{1}{6} j_{\max} T^3 \right] \\ + \frac{(v_0 + a_0 T - \frac{1}{2} j_{\max} T^2)^2}{2 |a_{\min,brake}|} \\ - \frac{v_f^2}{2 |a_{\max,brake}|} \end{array} \right]_+ \tag{7}$$

In the APB model, the safe distance is calculated based on the velocity and acceleration of the ego car, the velocity of the NMV, and the APB's three parameters that must be calibrated: minimum reasonable brake of the ego vehicle, maximum jerk of the ego vehicle, and maximum brake of the NMV, that is, $a_{min,brake}$, j_{max} and $a_{max,brake}$, respectively. Fig. 6 shows the relative distance and safe distance being compared at each simulation step, which is 0.1 s in this study. If the distance is safe, the APB system's status will be 0 and the car will travel at the driver-set velocity. If it is unsafe, the car will decelerate. The brake pressure at each step depends on the current status of the acceleration of the car. The brake pressure keeps increasing until it reaches $a_{min,brake}$.

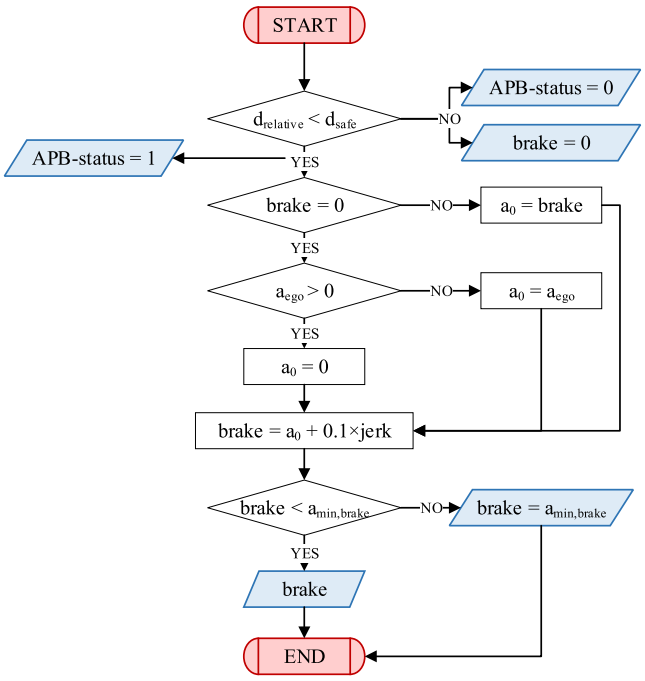

Fig. 6. Autonomous preventive braking algorithm.

The values of the three parameters, $a_{min,brake}$, j_{max} and $a_{max,brake}$ approximated the 50th, 75th, and 95th percentiles of the subject vehicle maximum deceleration and maximum jerk, and the NMV maximum deceleration shown in TABLE I. A total of 27 APB algorithms with the 27 combinations of values were studied, and are listed in TABLE III.

E. Evaluation Indicators

Evaluation of the autonomous braking algorithms considers both safety and conservativeness. Three indicators were used to evaluate driving safety: number of crashes, time-integrated time-to-collision (TIT), and driving volatility. Two indicators were used to evaluate conservativeness: TTC and relative distance at the time of brake activation.

1) Number of Crashes: Safety Indicator: Although no crashes actually occurred in the NDS safety critical events before extraction, the crashes were avoided because the drivers were successful at performing the evasive maneuvers that identified the events as SCEs. When an event was simulated and the autonomous braking algorithms, with their varying parameters, took control of the evasive maneuvers, avoidance of the crash in the simulation was not predetermined. An autonomous braking algorithm would still cause a crash if the brake was not applied in time or with sufficient strength.

2) Time-Integrated Time-to-Collision (TIT): Safety Indicator: Time-to-collision (TTC) is a widely used indicator of crash risk; however, the TTC is only measured at a given instant, so it cannot show how long the risky event lasts nor its severity within a given trip. The TIT indicator, in contrast, uses the integral of the time-to-collision profile of a trip to express the level of safety (in s^2) over a certain time period [43].

TABLE III
SUMMARY OF THE 27 APB ALGORITHMS UNDER STUDY

ID	$a_{min,brake}$ (m/s^2)	j_{max} (g/s)	$a_{max,brake}$ (m/s^2)	ID	$a_{min,brake}$ (m/s^2)	j_{max} (g/s)	$a_{max,brake}$ (m/s^2)	ID	$a_{min,brake}$ (m/s^2)	j_{max} (g/s)	$a_{max,brake}$ (m/s^2)
1	2.5	0.7	2.0	10	4.5	0.7	2.0	19	5.5	0.7	2.0
2	2.5	0.7	3.5	11	4.5	0.7	3.5	20	5.5	0.7	3.5
3	2.5	0.7	6.0	12	4.5	0.7	6.0	21	5.5	0.7	6.0
4	2.5	1.1	2.0	13	4.5	1.1	2.0	22	5.5	1.1	2.0
5	2.5	1.1	3.5	14	4.5	1.1	3.5	23	5.5	1.1	3.5
6	2.5	1.1	6.0	15	4.5	1.1	6.0	24	5.5	1.1	6.0
7	2.5	2.3	2.0	16	4.5	2.3	2.0	25	5.5	2.3	2.0
8	2.5	2.3	3.5	17	4.5	2.3	3.5	26	5.5	2.3	3.5
9	2.5	2.3	6.0	18	4.5	2.3	6.0	27	5.5	2.3	6.0

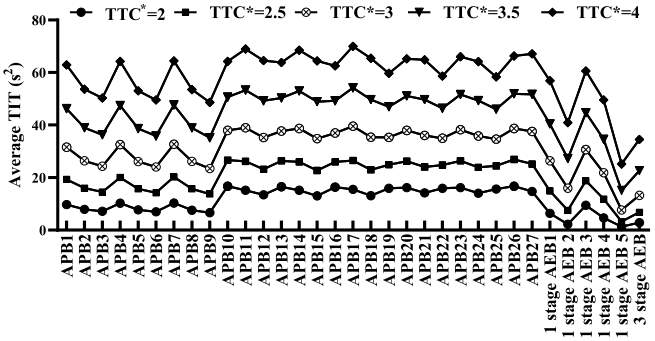

Fig. 7. Average TIT of the algorithms applying different TTC∗.

The TIT in a discrete time period is:

$$TIT = \sum_{t=1}^{T} (TTC* - TTC(t)) \times \tau_{SC} \quad \forall 0 \le TTC(t) \le TTC* \tag{8}$$

where TIT is the time-integrated TTC over time period T; $TTC(t)$ is the time-to-collision at time t; TTC^* is the TTC evaluation threshold (differing from TTC_b which is the activation threshold); and τ_{sc} is the time interval between the two simulation steps, which is set at 0.1 s. It is clear that the lower the TIT, the safer is the trip. As crashes are infrequent in the simulated SCEs, TIT as a safety indicator can provide a comprehensive analysis that considers both the duration and severity of the event in the context of a given trip.

The TTC threshold, on which TIT is based, varies from 2 s to 4 s in previous studies [44]–[47]. It has been found that a higher threshold is more sensitive in identifying risk conditions, while a lower threshold is helpful in investigating risk conditions with high severity [48]. However, the difference in safety evaluation when applying various TTC thresholds has not been shown to be significant [49]–[51]. This study applied 5 different TTC thresholds varying from 2 s to 4 s and calculated the average TIT values of the different autonomous braking algorithms. Fig. 7 shows that the relative average TIT values of the algorithms do not change with TTC thresholds, confirming previous findings that the TTC thresholds will not influence the algorithms' evaluation results. An intermediate TTC threshold of 3 s is used in the rest of the current analysis.

3) Driving Volatility (V_{dev}): Safety Indicator: A driver whose speed fluctuates greatly and who brakes sharply will disrupt the stability of his or her immediate traffic environment and increase the likelihood of rear-end collisions. Previous studies have found that driving volatility is significantly correlated with crash frequency and severity [52], [53], and can indicate the aggressiveness of a driver [54]. Therefore, an autonomous braking algorithm that maintains a low level of driving volatility is a vital safety feature for the surrounding vehicles. An easy and commonly used indicator for driving volatility is the standard deviation of speed [55]:

$$V_{dev} = \sqrt{\frac{1}{n-1} \sum_{t=1}^{T} (v_t - \bar{v})^2} \tag{9}$$

4) TTC When the Brake Is Activated (TTC_a): Conservativeness Indicator: As noted in relation to TIT, TTC is a good indicator of safety level at specific moments. While a brake activated when the TTC is long is considered as overly conservative and leading to frequent false alarms that disturb the driver, activation at a shorter TTC implies that the autonomous braking algorithm is less conservative, and will not brake until a real emergency.

5) Relative Distance When the Brake Is Activated (Dis_a): Conservativeness Indicator: The tested AEB algorithms are triggered by TTC, a time-related parameter, whereas the APB algorithm is triggered by safe distance, a distance-related parameter. To compare the conservativeness of these two kinds of algorithms equivalently, the relative distance between the subject vehicle and the NMV at the time of brake activation is also considered.

V. RESULTS

Before the three systems, one-stage AEB, three-stage AEB, and APB, can be compared, the best performing one-stage AEB and APB systems must be selected as multiple parameter combinations were evaluated for them. Since just one parameter combination of the three-stage AEB was under study, no selection was required.

A. Evaluation of One-Stage AEB Systems

As is shown in Fig. 8(a), in the five one-stage AEB algorithms (AEB 1-5, listed with their parameters in TABLE II), one crash occurred in AEB 1, in which deceleration (d_{one}) = 4.5 m/s^2 and the TTC threshold (TTC_b) = 2 s; there were no crashes in AEBs 2-5. Analysis of variance (ANOVA) was

TABLE IV
ANOVA RESULTS FOR TIT, V_{dev}, TTC_a AND Dis_a OF THE 5 ONE-STAGE AEB ALGORITHMS

Paired condition	TIT: time-integrated TTC		V_{dev}: driving volatility		TTC_a: TTC when the brake is activated		Dis_a: relative distance when the brake is activated	
	Difference	p-value	Difference	p-value	Difference	p-value	Difference	p-value
1 & 2	10.428*	<0.001	0.166*	<0.001	-0.371*	<0.001	-1.820*	<0.001
1 & 3	-4.238*	<0.001	-0.148*	<0.001	0.300*	<0.001	1.692*	<0.001
1 & 4	4.501*	<0.001	-0.049	0.089	0.000	/	0.000	/
1 & 5	18.752*	<0.001	0.220*	<0.001	-0.736*	<0.001	-3.518*	<0.001
2 & 3	-14.667*	<0.001	-0.314*	<0.001	0.671*	<0.001	3.512*	<0.001
2 & 4	-5.927*	<0.001	-0.214*	<0.001	0.371*	<0.001	1.820*	<0.001
2 & 5	8.324*	<0.001	0.055	0.155	-0.366*	<0.001	-1.698*	<0.001
3 & 4	8.739*	<0.001	0.099*	0.009	-0.300*	<0.001	-1.692*	<0.001
3 & 5	22.991*	<0.001	0.368*	<0.001	-1.037*	<0.001	-5.210*	<0.001
4 & 5	14.251*	<0.001	0.269*	<0.001	-0.736*	<0.001	-3.518*	<0.001

Note: * means p-value<0.05. Paired condition means that the two shown AEB algorithms are paired and compared; for example, 1 & 2 means the comparing AEB 1 and AEB 2.

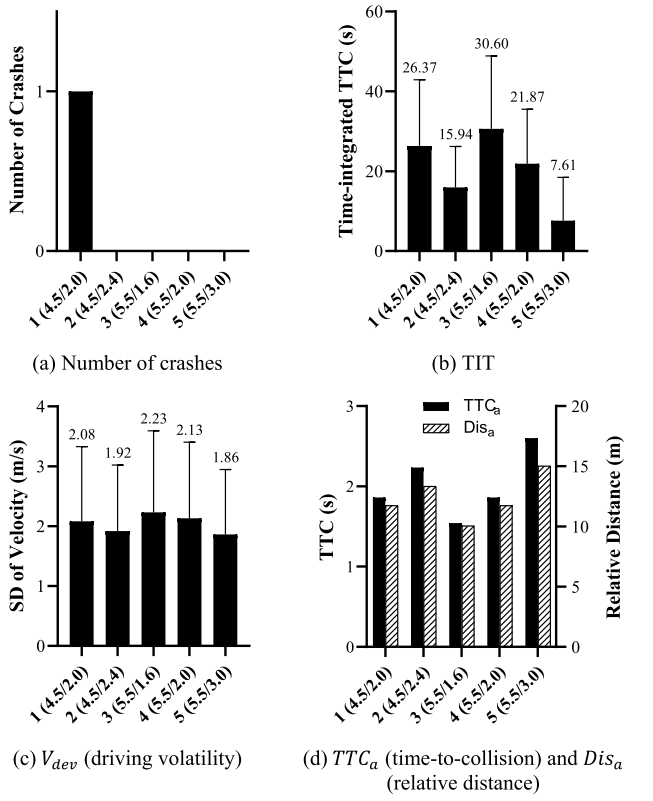

(a) Number of crashes (b) TIT

(c) V_{dev} (driving volatility) (d) TTC_a (time-to-collision) and Dis_a (relative distance)

Fig. 8. Number of crashes, TIT, V_{dev}, TTC_a and Dis_a of the 5 one-stage AEB algorithms.

conducted to determine whether the other four indicators of safety and conservativeness differed significantly with variations in deceleration and TTC threshold when the brake was activated. ANOVA results for TIT, driving volatility, TTC, and relative distance are shown in TABLE IV.

The bar charts in Fig. 8 illustrate the same four evaluation indicators. The 5 one-stage AEB algorithms are listed along the horizontal axis with their deceleration and TTC thresholds, respectively. The vertical axis in Fig. 8(b) shows the mean value and error bar of time-integrated TTC. The vertical axis in Fig. 8(c) shows the standard deviation of velocity, used to measure driving volatility. Fig. 8(d) shows TTC and relative distance together as they have the same trend. Taken together, the bar charts illustrate the following:

(1) With the variation of d_{one} and TTC_b, significant differences appeared in TIT ($F_{(4,428)} = 145.10$, $p < 0.001$), V_{dev} ($F_{(4,428)} = 26.15$, $p < 0.001$), TTC_a ($F_{(4,376)} = 392.24$, $p < 0.001$), and Dis_a ($F_{(4,428)} = 150.87$, $p < 0.001$) in all five one-stage AEB algorithms.

(2) TIT and V_{dev} show the same trend in relation to TTC threshold: the two indicators increased with the decrease of TTC_b. When TTC_b decreases, the vehicle brakes later and thus is exposed for a longer period to the unsafe condition in which TTC is lower than the evaluation threshold TTC∗.

(3) The trends of TTC_a and Dis_a are consistent with TTC_b; AEB 3 brakes latest and AEB 5 brakes earliest (p<0.001).

To conclude, taking the number of crashes as the primary safety indicator, four of the five one-stage AEB algorithms (AEBs 2-5) have only slight differences in safety performance. One-stage AEB 3 was able to prevent crashes with short TTC triggering and relative distance, which may reduce wasted traffic capacity and be less likely to cause false alarms and driver annoyance. Of the one-stage AEB algorithms, AEB 3, calibrated with $d_{one} = 5.5\,\mathrm{m/s^2}$, $TTC_b = 1.6\,\mathrm{s}$, is therefore recommended.

B. Evaluation of the APB Systems

Twenty-seven APB algorithms with different combinations of the three parameters, that is, minimum reasonable brake of ego vehicle, maximum jerk of ego vehicle, and maximum possible brake of NMV, $a_{min,brake}$, j_{max}, and $a_{max,brake}$, respectively, were tested on the simulated SCEs. ANOVA was conducted to explore whether the changes in the values of the three parameters had significant main effects on safety performance and conservativeness, as shown by the five indicators. A series of post-hoc analyses, shown in TABLE V, were conducted to determine the differences in the five indicators under different parameter combinations. As is illustrated in Fig. 9(d),

TABLE V
POST-HOC ANALYSIS OF APB NUMBER OF CRASHES, TIT, V_{dev}, TTC_a AND Dis_a

Indicator		Paired condition of the parameters								
		$a_{min,brake}$			j_{max}			$a_{max,brake}$		
		2.5 & 4.5	2.5 & 5.5	4.5 & 5.5	0.7 & 1.1	0.7 & 2.3	1.1 & 2.3	2.0 & 3.5	2.0 & 6.0	3.5 & 6.0
# of crashes	Difference	-0.014	-0.044*	-0.030*	-0.006	-0.015	-0.009	0.042*	0.060*	0.017*
	p-value	0.4503	0.045	0.003	0.441	0.050	0.150	0.001	0.000	0.002
TIT	Difference	-9.797*	-9.117*	0.680	0.084	-0.162	-0.246	0.390	3.080*	2.690*
	p-value	<0.001	<0.001	0.118	0.645	0.442	0.140	0.285	0.001	<0.001
V_{dev},	Difference	-0.150*	-0.113	0.037	-0.018*	-0.026*	-0.007	-0.186*	-0.245*	-0.059*
	p-value	0.001	0.055	0.061	0.042	0.030	0.339	<0.001	<0.001	0.002
TTC_a	Difference	0.908*	1.148*	0.241*	0.164*	0.319*	0.155*	-0.236*	-0.361*	-0.125*
	p-value	<0.001	<0.001	<0.001	<0.001	<0.001	<0.001	<0.001	<0.001	<0.001
Dis_a	Difference	4.783*	6.310*	1.527*	0.882*	1.751*	0.869*	-1.271*	-1.907*	-0.636*
	p-value	<0.001	<0.001	<0.001	<0.001	<0.001	<0.001	<0.001	<0.001	<0.001

Note: * means p-value<0.05

TTC and relative distance have similar trends, so are discussed together.

1) Number of Crashes: As is illustrated in Fig. 9(a), crashes occurred in all the 27 APB algorithms, varying from 7 to 21 crashes in the 108 safety-critical events. ANOVA results showed significant main effects of $a_{min,brake}$ ($F_{(2,214)} = 3.29$, $p = 0.039$) and $a_{max,brake}$ ($F_{(2,214)} = 13.53$, $p < 0.001$) on number of crashes. Post-hoc analyses tested for the least significant difference (LSD) of crashes for each paired condition (TABLE V). Crashes occurred more frequently when the car braked at the highest level of deceleration ($a_{min,brake} = 5.5\text{m/s}^2$) than they did at the two lower values. The higher was the expected maximum deceleration of the NMV $a_{max,brake}$, the less often the crashes occurred.

2) TIT: ANOVA revealed significant main effects of $a_{min,brake}$ ($F_{(2,214)} = 38.03$, $p < 0.001$) and $a_{max,brake}$ ($F_{(2,214)} = 14.82$, $p < 0.001$) on TIT. As can be seen in Fig. 9(b), TIT was significantly lower in the first 9 APB algorithms, in which the ego vehicle braked the least ($a_{min,brake} = 2.5\ \text{m/s}^2$). Post-hoc analysis showed that TIT was lower when $a_{max,brake} = 6\ \text{m/s}^2$ than with the two lower values (p<0.001). j_{max} had no significant main effect on either number of crashes or TIT.

3) Driving Volatility: ANOVA revealed significant main effects of $a_{min,brake}$($F(2,212) = 6.29$, $p = 0.002$), j_{max} ($F_{(2,212)} = 3.87$, $p = 0.022$), and $a_{max,brake}$($F_{(2,212)} = 41.68$, $p < 0.001$) on driving volatility V_{dev}. Post-hoc analysis showed that the vehicle speed was more stable when $j_{max} = 0.7$ g/s than at 1.1 g/s ($p = 0.042$) or 2.3 m/s ($p = 0.030$), which makes sense because the lower the j_{max}, the smoother the vehicle decelerates and therefore causes less fluctuation in traffic flow. Volatility also decreased with the decrease in $a_{max,brake}$, as a slighter brake of the lead NMV reduced its influence on the ego vehicle.

4) TTC and Relative Distance When Brake Is Activated: ANOVA revealed significant main effects of $a_{min,brake}$ ($F_{(2,162)} = 219.431$, $p < 0.001$), j_{max} ($F_{(2,162)} = 590.167$, $p < 0.001$), and $a_{max,brake}$ ($F_{(2,162)} = 86.411$, $p < 0.001$) on time-to-collision TTC_a. Significant main effects on Dis_a were also seen: $a_{min,brake}$ ($F_{(2,162)} = 129.106$, $p < 0.001$), j_{max} ($F_{(2,162)} = 473.492$, $p < 0.001$), and $a_{max,brake}$ ($F_{(2,162)} = 77.739$, $p < 0.001$). Post-hoc analysis showed that the larger the $a_{min,brake}$ and j_{max}, and the smaller the $a_{max,brake}$, the later the ego vehicle started to brake and the closer the two vehicles were when the brake was activated.

TABLE VI
NUMBER OF CRASHES WITH ONE-STAGE AEB 3, THREE-STAGE AEB, AND APB 12

	One-stage AEB 3	Three-stage AEB	APB 12
Number of crashes	0	1	7

Safety, of course, is the primary concern of an autonomous braking algorithm, and none of the APB algorithms succeeded in preventing all crashes. Three algorithms, APB 2, APB 3, and APB 12, had seven, the fewest number of crashes. Among the three, APB 12 was less conservative than the other two, as indicated by its lower TTC_a and Dis_a, and was thus selected for the overall comparison between the three different system types.

C. Comparison of the Three Autonomous Braking Systems

The objective of this section is to discover the differences between the one-stage AEB, three-stage AEB, and APB systems, and thereby determine the optimum autonomous braking system for SCEs between motorized and non-motorized vehicles. The previous two sections demonstrated that APB 12 and one-stage AEB 3 outperformed the other algorithms of their system type, and were thus selected to represent that type. There is only one parameter combination of three-stage AEB.

As is shown in TABLE VI, among the three selected systems, only one-stage AEB was able to prevent all crashes; one crash occurred in three-stage AEB, and seven occurred in APB 12.

Distributions of the four other indicators, TIT, V_{dev}, TTC_a, and Dis_a, for the 108 simulated SCEs are shown in the form of histograms in VI. 10, where *frequency* in the vertical axis indicates number of events. As some of the systems' bars overlap in the histograms, fitted distribution curves are plotted to help understand the changing trends. Taken together with the AVONA results in TABLE VII, the following can be seen:

(1) One-stage AEB, three-stage AEB, and APB have significant differences in TIT ($F_{(2,214)} = 57.60$, $p < 0.001$).

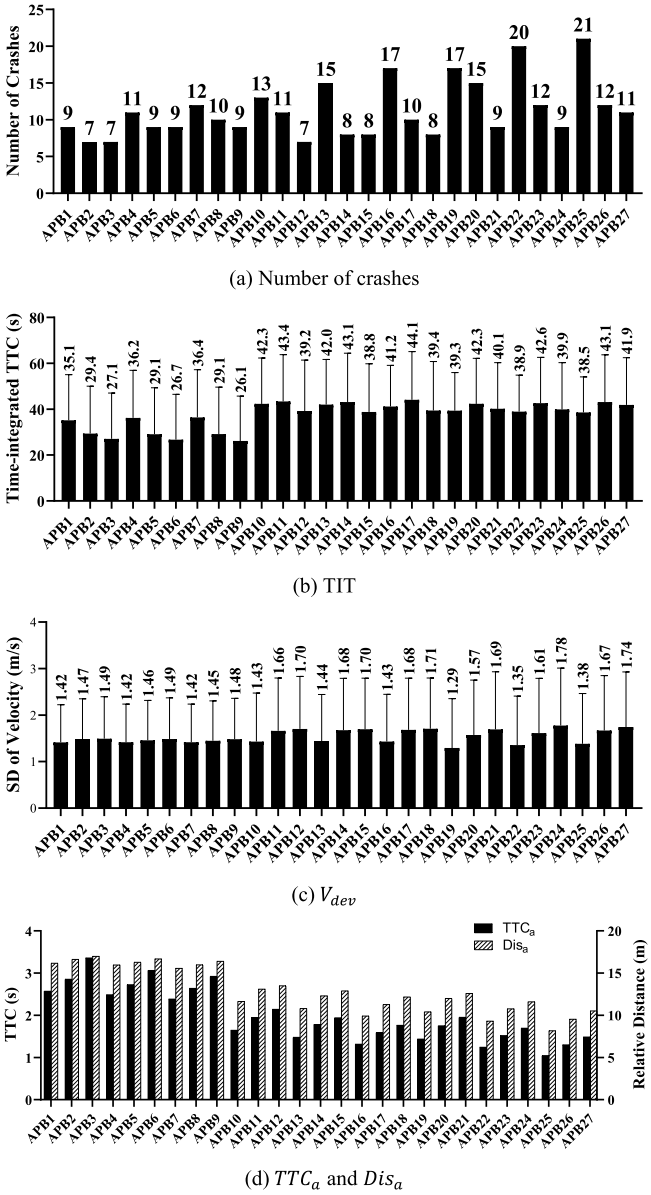

(a) Number of crashes

(b) TIT

(c) V_{dev}

(d) TTC_a and Dis_a

Fig. 9. Number of crashes, TIT, V_{dev}, TTC_a and Dis_a of the 27 APB algorithm.

TABLE VII

ANOVA RESULTS FOR TIT, V_{dev}, TTC_a AND Dis_a OF THE THREE BRAKING SYSTEMS

Indicator		Paired condition		
		1-stage AEB & 3-stage AEB	1-stage AEB & APB	3-stage AEB & APB
TIT	Difference	17.399*	-4.608*	-22.007*
	p-value	<0.001	<0.001	<0.001
V_{dev},	Difference	-0.654*	0.528*	1.182*
	p-value	<.001	<0.001	<0.001
TTC_a	Difference	-1.093*	-0.582*	0.511*
	p-value	<0.001	<0.001	<0.001
Dis_a	Difference	-6.414*	13.698*	2.716*
	p-value	<0.001	<0.001	<0.001

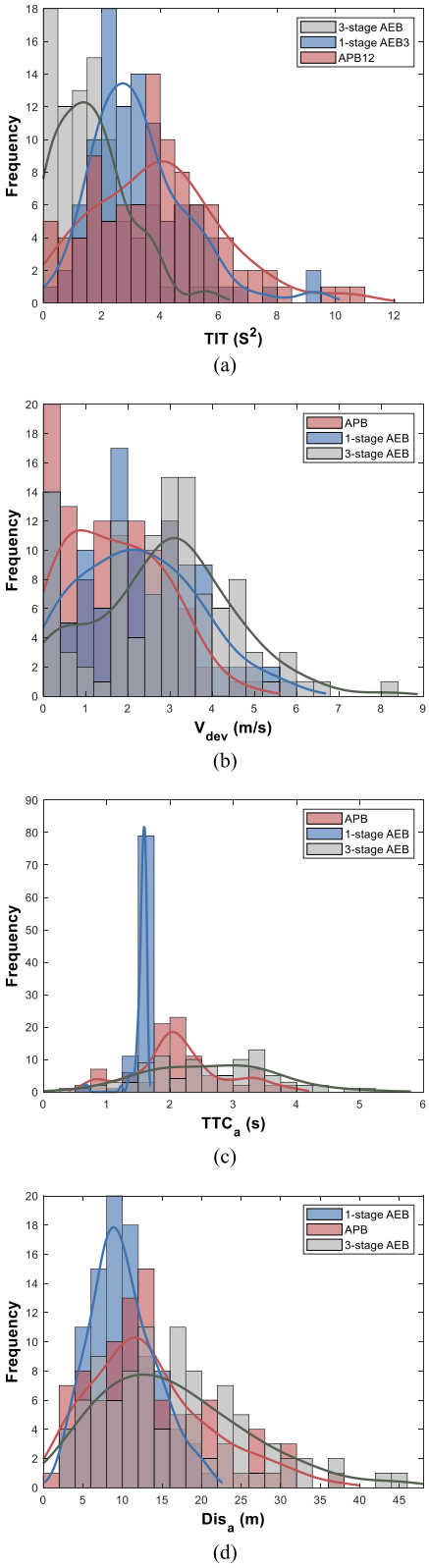

(a)

(b)

(c)

(d)

Fig. 10. Histograms and fitted distribution curves of TIT, V_{dev}, TTC_a and Dis_a.

The Fig. 10(a) histogram's distribution of one-stage AEB and three-stage AEB are more right-skewed than that of APB, and the mean TIT of APB is 4.61 s^2 larger than that of one-stage AEB, and 22.01 s^2 larger than three-stage AEB.

(2) The three systems have significant differences in V_{dev} ($F_{(2,214)} = 109.85$, $p < 0.001$). The histogram's

distributions are more dispersed in Fig. 10(b) than in Fig. 10(a), but it is still clear that APB produces lower driving volatility, while three-stage AEB produces higher volatility.

(3) The systems have significant differences in TTC_a ($F_{(2,180)} = 95.06$, $p < 0.001$) and Dis_a($F_{(2,180)} = 65.28$, $p < 0.001$). In Fig. 10(c), the TTC_a of one-stage AEB is centralized within 1.5 s and 1.75 s because the system's threshold TTC_b is 1.6 s, whereas the TTC_a of APB and the three-stage AEB are more dispersed because their thresholds are not fixed values. The Dis_a distribution of one-stage AEB shown in Fig. 10(d) is also more right-skewed than the other two systems, indicating that one-stage AEB brakes later and at a closer relative distance.

Overall, even though the APB system has lowest driving volatility, it shows the least adequate safety performance as it has more crashes and higher TIT than the other two systems. One-stage AEB succeeded in preventing all crashes, and has better driving stability (less volatility) than three-stage AEB. Additionally, it brakes later and may therefore cause fewer false alarms. Considering both safety and conservativeness, the one-stage AEB system with $d_{one} = 5.5$ m/s^2, $TTC_b = 1.6\,s$ shows the best performance.

VI. Summary and Discussion

A. Evaluation of One-Stage AEB, Three-Stage AEB, and APB

In Section V, the safety performance and conservativeness of 5 one-stage AEB algorithms, 1 three-stage AEB algorithm and 27 APB algorithms were evaluated. One-stage AEB 3, which was calibrated at $d_{one} = 5.5$ m/s^2, $TTC_b = 1.6$ s, was selected to represent the one-stage AEB system as it was able to prevent all crashes without braking prematurely. Only one group of parameters ($d^1_{three} = 2.5$ m/s^2, $d^2_{three} = 4.5\ m/s^2$ and $d^3_{three} = 5.5\ m/s^2$) were tested on the three-stage AEB system, for which the results showed that the system would cause one crash. Seven was the fewest number of crashes caused by any of the 27 APB algorithms. APB 12, calibrated with $a_{min,brake} = 4.5$m/s^2, $j_{max} = 0.7$ g/s, and $a_{max,brake} = 6$m/s^2, was one of three APB algorithms that caused seven crashes; as it braked latest, and was therefore least conservative, it was selected for comparison with the two AEB systems.

The comparison revealed that the APB system's safety performance was inferior to that of the two AEB systems in that it caused a greater number of crashes and also had higher TIT. However, APB's jerk-bounded braking profile did reduce braking intensity, and thereby generated low driving volatility. An autonomous braking system with lower volatility will cause less impact to the vehicle following it, and less fluctuation in the traffic flow. As has been claimed [17], one of the aims of APB is to not compromise the traffic throughput, which this study has demonstrated to be achievable.

One-stage AEB was shown to be the least conservative system, braking latest, while three-stage AEB brakes earliest, and thus may lead to frequent false alarms. This study demonstrated that for safety-critical events, one-stage AEB can prevent crashes by applying a moderate deceleration with a relatively small TTC threshold. The APB system, while somewhat less conservative, is not as safe as Shalev-Shwartz supposed it to be [17]. As was shown in Fig. 9(d), by the increases in $a_{min,brake}$ and j_{max}, the brake is activated late and is more likely to cause a crash.

B. Impact on APB Safe Distance and Trigger Time of Ego Vehicle Minimum Reasonable Brake and NMV Maximum Possible Brake

In Eq. 7, safe distance in the APB model was defined as the difference in distance that the lead and following vehicles each require to reach a full stop. For the subject following vehicle, the larger its minimum reasonable brake $a_{min,brake}$ and maximum jerk j_{max}, the better is its braking ability and thus the shorter distance it needs to reach a full stop. A larger $a_{max,brake}$ for the lead NMV indicates that the event is more critical and the lead vehicle will reach a full stop sooner, which leads to a shorter full brake distance for the NMV. Consequently, the increase of the subject vehicle's $a_{min,brake}$ and j_{max} will decrease the safe distance while the increase of the NMV's $a_{max,brake}$ will increase safe distance.

In Section V.B, results showed that crashes occurred more frequently when the ego vehicle had better braking ability (larger $a_{min,brake}$), and less frequently when the event was more critical (larger $a_{max,brake}$), both of which are contrary to our expectations. In Fig. 11, the safe distance and actual headway of two randomly selected events are plotted using the baseline APB algorithm (APB 1) and two other algorithms, one with larger $a_{min,brake}$ (APB 19) and one with larger $a_{max,brake}$ (APB 3). The solid lines represent the safe distance, the dashed line the actual headway, and the dots represent the brake activation time.

In both events, APB 19, the APB algorithm with larger $a_{min,brake}$, brakes later than the APB 1 baseline algorithm, as APB 19 provides the vehicle with stronger brake ability, while APB 3, the algorithm with larger $a_{max,brake}$, brakes earlier as it supposes the events to be more critical.

It should also be noticed in Fig. 11 that the safe distance is not a smooth line, but fluctuates across the headway from time to time. The fluctuation is mainly caused by changes in velocity and acceleration: 1) the vehicle decelerates when the headway is smaller than the safe distance; 2) this decrease of velocity and acceleration makes it easier for the following vehicle to reach a full stop, thereby reducing the safe distance; 3) once the safe distance drops below headway, the vehicle will stop the braking process and start to accelerate; however, little difference between headway and safe distance is evident at that point; 4) headway soon becomes smaller again than safe distance, and the vehicle again begins to decelerate. This fluctuation interrupts the continuous deceleration process and raises another problem. The safe distance is calculated under the assumption that the vehicle will continue decelerating until the distance becomes totally safe, but instead, the vehicle starts to accelerate as soon as the safe distance exceeds headway. Thus, the observation that crashes occurred more frequently when the ego vehicle had better braking ability, and less frequently when the event was more critical, is explained:

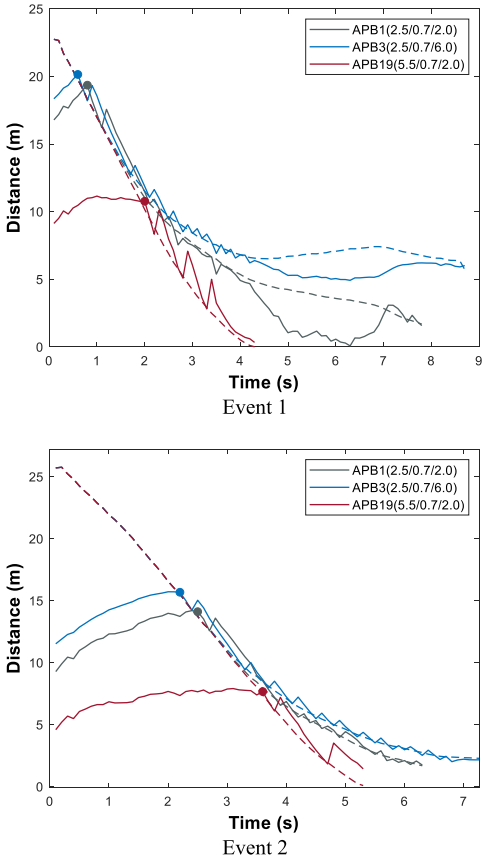

Fig. 11. Safe distance and headway of APB algorithms with different $a_{min,brake}$ and $a_{max,brake}$.

the APB 3 vehicle brakes earlier for more critical events, and so has more time to react, but the strong but late braking of the APB 19 vehicle will easily fail to reach a full stop, which may tend to cause more crashes under this condition of fluctuation.

C. Impact of Triggering Criteria

The three autonomous braking systems are triggered by different criteria, which may be responsible for some of the results. The two AEB systems that were tested are both triggered by time while the APB system is triggered by distance. To illustrate the difference, Fig. 12 shows two randomly selected events, with the horizontal axis indicating the event's progression in time, and the vertical axis indicating time-to-collision for the AEB systems or headway for APB, with the changes represented by the black lines. The vertical blue dashed lines are the brake activation times. One-stage AEB is triggered by a fixed 1.6-s TTC threshold shown by the red horizontal line in Fig. 12(a) and (d), while three-stage AEB is triggered by three speed-related stopping times: the yellow, orange and red lines in Fig. 12(b) and (d) are the stopping times when deceleration values are 2.5 m/s^2, 4.5 m/s^2, and 5.5 m/s^2, respectively. The APB safe distance trigger is more complicated as it not only involves three parameters, the values of which are unknown, but also relies on real-time speed and acceleration.

In both AEB systems, the brake is triggered when TTC drops below the threshold line, and the entire deceleration process is completed once the TTC increases beyond the threshold. As was explained in Section VI.B, however, the APB safe distance fluctuates with the changing velocity and acceleration of the vehicle. Such repeated accelerations and decelerations erode the reserved braking distance and increase the possibility of a crash.

In summary, the deceleration process of the time-triggered AEB systems is more consistent and reliable, while the

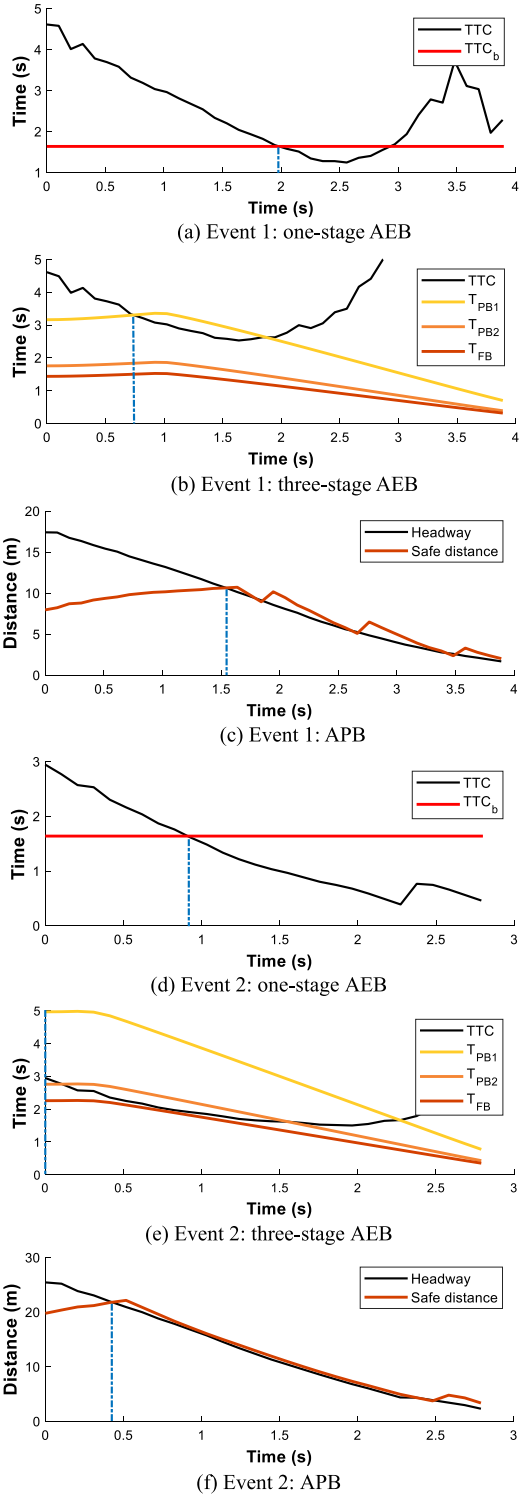

Fig. 12. Triggering criteria for the three systems.

APB deceleration process triggered by safe distance is more unpredictable due to the change of the three parameters and real-time kinetic parameter values.

VII. Conclusion

To explore ways to ensure the traffic safety of non-motorized vehicles in an autonomous driving environment, this study calibrated and compared three autonomous braking systems: one-stage AEB, three-stage AEB, and APB. A total of 108 longitudinal safety-critical events between motorized and non-motorized vehicles were extracted from the Shanghai Naturalistic Driving Study and recreated in the MATLAB simulation platform. One three-stage AEB algorithm, five one-stage AEB algorithms, and twenty-seven APB algorithms with different combinations of parameter values were tested on the safety-critical events. The algorithms were evaluated for safety performance (indicators: number of crashes, TIT, driving volatility) and conservativeness (indicators: TTC and relative distance when brake is activated) in order to identify the optimal parameter combinations in each system. The results showed that:

(1) One-stage AEB with deceleration and time-to-collision thresholds of $d_{one} = 5.5$ m/s^2, $TTC_b = 1.6$ s can avoid all crashes, and is the least conservative among the 5 one-stage AEB algorithms.
(2) Three-stage AEB with deceleration and time-to-collision thresholds of $d^1_{three} = 2.5\ m/s^2$, $d^2_{three} = 4.5\ m/s^2$ and $d^3_{three} = 5.5\ m/s^2$ caused one crash.
(3) APB with ego vehicle minimum reasonable brake, ego vehicle maximum jerk, and NMV maximum possible brake of $a_{min,brake} = 4.5$m/s^2, $j_{max} = 0.7$ g/s, and $a_{max,brake} = 6$m/s^2, respectively, caused the fewest crashes and is the least conservative among the 27 APB algorithms.

The comparison between the above three calibrated systems demonstrated that one-stage AEB has the best safety performance and is the least conservative. Although the APB system has the best driving stability and therefore causes less fluctuation in the traffic flow, it was shown to cause the most crashes. Further analysis of the APB brake pattern revealed that the crashes were likely the result of fluctuating safe distance combined with the fact that larger $a_{min,brake}$ and j_{max} postpone brake activation time. Comparison of the triggering criteria suggested that the time-triggered brake process of the AEB systems may be more consistent and reliable than the distance-triggered process of the APB system.

Two main contributions have been made by this study. First, by calibrating the parameters of the autonomous braking systems with SCEs between motorized and non-motorized vehicles, it was shown that a one-stage AEB with low deceleration is the best of the tested systems at defusing the danger of SCEs. Second, the APB system was calibrated for the first time with naturalistic driving data and its effectiveness was evaluated. The APB's safety performance was not as good as expected, as the trigger time and safe distance criteria are easily affected by the pre-defined parameters and changing kinetic parameters.

TABLE VIII
Glossary of Terms

Abbreviation	Explanation
AEB	Autonomous emergency braking
APB	Automatic preventive braking
SCE	Safety-critical event
AV	Automated vehicles
NMV	Non-motorized vehicles
ADAS	Advanced driving assistant systems
TTC	Time-to-collision
RSS	Responsibility-Sensitive Safety
NDS	Naturalistic driving study
SH-NDS	Shanghai Naturalistic Driving Study
FCW	Forward collision warning
GPS	The Global Positioning System
SHRP2	The second Strategic Highway Research Program
EuroNCAP	The European New Car Assessment Programme
CATS	Cyclist-AEB testing system
PCW	Pedestrian and cyclist warning
MIO	Most important object
ADAC	Allgemeiner Deutscher Automobil-Club
TIT	Time-integrated time-to-collision
ANOVA	Analysis of variance
LSD	Least significant difference

This study has some limitations. Only 108 SCEs were tested, and only longitudinal scenarios, that is, no crossing or turning scenarios, were considered. Future research should investigate and analyze a greater number of events with various types of scenarios. Although it was demonstrated that smoother deceleration would be preferable in the safety-critical event, a method to distinguish the events' severity level in real-life driving was not, in the current study, given attention. Similarly, the identification of APB modeling issues that may cause crashes was merely speculation. It will be left to future studies to consider how to improve the system to take advantage of the APB's driving stability benefit. Similarly, future research can use our results of longitudinal SCEs to investigate their disproportion in the Shanghai study area.

Appendix

The terminologies and abbreviations in the paper are summarized in TABLE VIII.

References

[1] D. González, J. Pérez, V. Milanés, and F. Nashashibi, "A review of motion planning techniques for automated vehicles," *IEEE Trans. Intell. Transp. Syst.*, vol. 17, no. 4, pp. 1135–1145, Apr. 2016.
[2] X. Li *et al.*, "A new benchmark for vision-based cyclist detection," in *Proc. IEEE Intell. Vehicles Symp. (IV)*, Gothenburg, Sweden, Jun. 2016, pp. 1028–1033.
[3] Xinhuanet. (Nov. 12, 2019). *The Number of Bicycles in China is Nearly 400 Million, Ranking First in the World*. [Online]. Available: http://www.xinhuanet.com/fortune/2019-11/22/c_1125264380.htm
[4] *Annual Report on Traffic Accidents Statistics (Year 2015)*, Traffic Manage. Bur. Public Secur. Ministry, Traffic Manage. Res. Inst. Ministry Public Security, Wuxi, China, 2016.
[5] E. Krug *et al.*, "Powered two- and three-wheeler safety: A road safety manual for decision-makers and practitioners," World Health Org., Geneva, Switzerland, Tech. Rep., 2017.

[6] *Road Safety Annual Report 2019 Sweden*, Int. Transp. Forum, Paris, France, 2020.

[7] B. Fildes *et al.*, "Effectiveness of low speed autonomous emergency braking in real-world rear-end crashes," *Accident Anal. Prevention*, vol. 81, pp. 24–29, Aug. 2015.

[8] Y. Li, L. Xing, W. Wang, H. Wang, C. Dong, and S. Liu, "Evaluating impacts of different longitudinal driver assistance systems on reducing multi-vehicle rear-end crashes during small-scale inclement weather," *Accident Anal. Prevention*, vol. 107, pp. 63–76, Oct. 2017.

[9] J. Saadé, "Autonomous emergency braking AEB (pedestrians & cyclists)," Eur. Road Saf. Decis. Support Syst., Tech. Rep., 2017.

[10] O. O. D. Camp, S. van Montfort, J. Uittenbogaard, and J. Welten, "Cyclist target and test setup for evaluation of cyclist-autonomous emergency braking," *Int. J. Automot. Technol.*, vol. 18, no. 6, pp. 1085–1097, Dec. 2017.

[11] E. Rosén, "Autonomous emergency braking for vulnerable road users," in *Proc. Int. Res. Council Biomech. Injury (IRCOBI)*, 2013, pp. 618–627.

[12] Y. Zhao, D. Ito, and K. Mizuno, "AEB effectiveness evaluation based on car-to-cyclist accident reconstructions using video of drive recorder," *Traffic Injury Prevention*, vol. 20, no. 1, pp. 100–106, Mar. 2019.

[13] M. Edwards, A. Nathanson, and M. Wisch, "Estimate of potential benefit for Europe of fitting autonomous emergency braking (AEB) systems for pedestrian protection to passenger cars," *Traffic Injury Prevention*, vol. 15, no. sup1, pp. S173–S182, Oct. 2014.

[14] Y.-L. Chen, K.-Y. Shen, and S.-C. Wang, "Forward collision warning system considering both time-to-collision and safety braking distance," in *Proc. IEEE 8th Conf. Ind. Electron. Appl. (ICIEA)*, Jun. 2013, pp. 972–977.

[15] D. H. Lee, S. K. Kim, C. S. Kim, and K. S. Huh, "Development of an autonomous braking system using the predicted stopping distance," *Int. J. Automot. Technol.*, vol. 15, no. 2, pp. 341–346, 2014.

[16] E. Coelingh, A. Eidehall, and M. Bengtsson, "Collision warning with full auto brake and pedestrian detection—A practical example of automatic emergency braking," in *Proc. 13th Int. IEEE Conf. Intell. Transp. Syst. (ITSC)*, Sep. 2010, pp. 155–160.

[17] S. Shalev-Shwartz, S. Shammah, and A. Shashua, "Vision zero: On a provable method for eliminating roadway accidents without compromising traffic throughput," 2018, *arXiv:1901.05022*.

[18] X. Xu, X. Wang, X. Wu, O. Hassanin, and C. Chai, "Calibration and evaluation of the responsibility-sensitive safety model of autonomous car-following maneuvers using naturalistic driving study data," *Transp. Res. C, Emerg. Technol.*, vol. 123, pp. 1–17, Feb. 2021.

[19] S. Liu *et al.*, "Calibration and evaluation of responsibility-sensitive safety (RSS) in automated vehicle performance during cut-in scenarios," *Transp. Res. C, Emerg. Technol.*, vol. 125, pp. 1–15, Apr. 2021.

[20] B. Gassmann *et al.*, "Towards standardization of AV safety: C++ library for responsibility sensitive safety," in *Proc. IEEE Intell. Vehicles Symp. (IV)*, Jun. 2019, pp. 2265–2271.

[21] P. Koopman, B. Osyk, and J. Weast, "Autonomous vehicles meet the physical world: RSS, variability, uncertainty, and proving safety (expanded version)," 2019, *arXiv:1911.01207*.

[22] F. Char, T. Serre, S. Compigne, and P. P. Guillen, "Car-to-cyclist forward collision warning effectiveness evaluation: A parametric analysis on reconstructed real accident cases," *Int. J. Crashworthiness*, vol. 27, no. 1, pp. 34–43, 2022.

[23] H. Jeppsson and N. Lubbe, "Simulating automated emergency braking with and without torricelli vacuum emergency braking for cyclists: Effect of brake deceleration and sensor field-of-view on accidents, injuries and fatalities," *Accident Anal. Prevention*, vol. 142, pp. 1–15, Jul. 2020.

[24] Q. Liu, X. Wang, X. Wu, Y. Glaser, and L. He, "Crash comparison of autonomous and conventional vehicles using pre-crash scenario typology," *Accident Anal. Prevention*, vol. 159, Sep. 2021, Art. no. 106281.

[25] M. Zhu, X. Wang, and Y. Wang, "Human-like autonomous car-following model with deep reinforcement learning," *Transp. Res. C, Emerg. Technol.*, vol. 97, pp. 348–368, Dec. 2018.

[26] T. A. Dingus *et al.*, "The 100-car naturalistic driving study phase II—Results of the 100-car field experiment," U.S. Dept. Transp., Nat. Highway Traffic Saf. Admin., Washington, DC, USA, Tech. Rep. DOT HS 810 593, 2006.

[27] F. Guo, S. G. Klauer, J. M. Hankey, and T. A. Dingus, "Near crashes as crash surrogate for naturalistic driving studies," *Transp. Res. Rec., J. Transp. Res. Board*, vol. 2147, no. 1, pp. 66–74, Jan. 2010.

[28] K.-F. Wu and P. P. Jovanis, "Crashes and crash-surrogate events: Exploratory modeling with naturalistic driving data," *Accident Anal. Prevention*, vol. 45, pp. 507–516, Mar. 2012.

[29] F. Guo and Y. Fang, "Individual driver risk assessment using naturalistic driving data," *Accident Anal. Prevention*, vol. 61, no. 6, pp. 3–9, Dec. 2013.

[30] *Comparative Test of Advanced Emergency Braking Systems*, Allgemeiner Deutscher Automobil-Club (ADAC), Landsberg, Germany, 2013.

[31] K. D. Kusano and H. C. Gabler, "Safety benefits of forward collision warning, brake assist, and autonomous braking systems in rear-end collisions," *IEEE Trans. Intell. Transp. Syst.*, vol. 13, no. 4, pp. 1546–1555, Dec. 2012.

[32] J. B. Cicchino, "Effectiveness of forward collision warning and autonomous emergency braking systems in reducing front-to-rear crash rates," *Accident Anal. Prevention*, vol. 99, pp. 142–152, Feb. 2016.

[33] M.-K. Park, S.-Y. Lee, C.-K. Kwon, and S.-W. Kim, "Design of pedestrian target selection with funnel map for pedestrian AEB system," *IEEE Trans. Veh. Technol.*, vol. 66, no. 5, pp. 3597–3609, May 2017.

[34] M. Zhao, H. Wang, J. Chen, X. Xu, and Y. He, "Method to optimize key parameters and effectiveness evaluation of the AEB system based on rear-end collision accidents," *SAE Int. J. Passenger Cars, Electron. Electr. Syst.*, vol. 10, no. 2, pp. 310–317, 2017.

[35] Y. Peng, W. Yu, X. Wang, Q. Xu, H. Wang, and W. Wu, "AEB effectiveness research methods based on reconstruction results of truth vehicle-to-TW accidents in China," *Proc. Inst. Mech. Eng. D, J. Automobile Eng.*, vol. 235, no. 7, pp. 2029–2039, Jun. 2021.

[36] S. Shalev-Shwartz, S. Shammah, and A. Shashua, "On a formal model of safe and scalable self-driving cars," 2017, *arXiv:1708.06374*.

[37] K. Mattas *et al.*, "Fuzzy surrogate safety metrics for real-time assessment of rear-end collision risk. A study based on empirical observations," *Accident Anal. Prevention*, vol. 148, pp. 1–10, Dec. 2020.

[38] Virginia Tach Transportation Institute. *Laboratories and Data Acquisition Systems*. Accessed: Jan. 2022. [Online]. Available: https://www.vtti.vt.edu/facilities/labs-das.html

[39] *Mobileye C2-270 User Manual*. Accessed: Jan. 2022. [Online]. Available: http://c2sec.com.sg/Files/Mobileye%20C2-270%20User Manual.pdf

[40] J. M. Hankey, M. A. Perez, and J. A. McClafferty, "Description of the SHRP 2 naturalistic database and the crash, near-crash, and baseline data sets," Virginia Tech Transp. Inst., Blacksburg, VA, USA, Tech. Rep., Apr. 2016. [Online]. Available: http://hdl.handle.net/10919/70850.

[41] Y. G. Glaser, F. Guo, Y. Fang, B. Deng, and J. Hankey, "Investigate moped-car conflicts in China using a naturalistic driving study approach," *J. Saf. Res.*, vol. 63, pp. 171–175, Dec. 2017.

[42] J. Duan *et al.*, "Driver braking behavior analysis to improve autonomous emergency braking systems in typical Chinese vehicle-bicycle conflicts," *Accident Anal. Prevention*, vol. 108, pp. 74–82, Nov. 2017.

[43] M. M. Minderhoud and P. H. Bovy, "Extended time-to-collision measures for road traffic safety assessment," *Accident Anal. Prevention*, vol. 33, no. 1, pp. 89–97, Jan. 2001.

[44] R. van der horst and J. Hogema, "Time-to-collision and collision avoidance systems," presented at the 6th ICTCT Workshop Salzburg, 1994.

[45] Q. Meng and X. Qu, "Estimation of rear-end vehicle crash frequencies in urban road tunnels," *Accident Anal. Prevention*, vol. 48, pp. 254–263, Sep. 2012, doi: 10.1016/j.aap.2012.01.025.

[46] Z. Li, Y. Li, P. Liu, W. Wang, and C. Xu, "Development of a variable speed limit strategy to reduce secondary collision risks during inclement weathers," *Accident Anal. Prevention*, vol. 72, pp. 134–145, Nov. 2014, doi: 10.1016/j.aap.2014.06.018.

[47] Y. Li, Z. Li, H. Wang, W. Wang, and L. Xing, "Evaluating the safety impact of adaptive cruise control in traffic oscillations on freeways," *Accident Anal. Prevention*, vol. 104, pp. 137–145, Jul. 2017, doi: 10.1016/j.aap.2017.04.025.

[48] X. Shi, Y. D. Wong, M. Z. F. Li, and C. Chai, "Key risk indicators for accident assessment conditioned on pre-crash vehicle trajectory," *Accident Anal. Prevention*, vol. 117, pp. 346–356, Aug. 2018, doi: 10.1016/j.aap.2018.05.007.

[49] Y. Tu, W. Wang, Y. Li, C. Xu, T. Xu, and X. Li, "Longitudinal safety impacts of cooperative adaptive cruise control vehicle's degradation," *J. Saf. Res.*, vol. 69, pp. 177–192, Jun. 2019, doi: 10.1016/j.jsr.2019.03.002.

[50] M. S. Rahman and M. Abdel-Aty, "Longitudinal safety evaluation of connected vehicles' platooning on expressways," *Accident Anal. Prevention*, vol. 117, pp. 381–391, Aug. 2018, doi: 10.1016/j.aap.2017.12.012.

[51] Y. Li, H. Wang, W. Wang, S. Liu, and Y. Xiang, "Reducing the risk of rear-end collisions with infrastructure-to-vehicle (I2V) integration of variable speed limit control and adaptive cruise control system," *Traffic Injury Prevention*, vol. 17, no. 6, pp. 597–603, Aug. 2016, doi: 10.1080/15389588.2015.1121384.

[52] R. Arvin, M. Kamrani, and A. J. Khattak, "Examining the role of speed and driving stability on crash severity using SHRP2 naturalistic driving study data," in *Proc. Transp. Res. Board 98th Annu. Meeting Res. Board*, Washington, DC, USA, 2019, p. 8.
[53] A. J. Khattak and B. Wali, "Analysis of volatility in driving regimes extracted from basic safety messages transmitted between connected vehicles," *Transp. Res. C, Emerg. Technol.*, vol. 84, pp. 48–73, Nov. 2017.
[54] M. Kamrani, R. Arvin, and A. J. Khattak, "The role of aggressive driving and speeding in road safety: Insights from SHRP2 naturalistic driving study data," in *Proc. Transp. Res. Board 98th Annu. Meeting Res. Board*, Washington, DC, USA, 2019, p. 6.
[55] M. Kamrani, R. Arvin, and A. J. Khattak, "Extracting useful information from basic safety message data: An empirical study of driving volatility measures and crash frequency at intersections," *Transp. Res. Rec., J. Transp. Res. Board*, vol. 2672, no. 38, pp. 290–301, Dec. 2018.

Weixuan Zhou received the B.Sc. degree in transportation engineering from Tongji University, Shanghai, China, in 2020, where she is currently pursuing the M.A. degree in transportation engineering. Her research interests include traffic safety analysis, autonomous vehicle, advanced driving assistant systems (ADAS), vulnerable road users, and naturalistic driving study.

Xuesong Wang received the Ph.D. degree from the University of Central Florida, Orlando, FL, USA, in 2006. In Fall 2008, he joined Tongji University, Shanghai, China, where he is currently a Professor at the School of Transportation Engineering. His research interests include safety assessment of autonomous vehicles, naturalistic driving study, driving behavior analysis, traffic safety analysis, safety evaluation of roadway design, and transportation safety planning. On these topics, he has authored or coauthored over 350 papers in journals and conferences. He is a member of the TRB Standing Committees on Transportation in the Developing Countries (AME40), Safety Performance Analysis (ACS20), and Road User Measurement and Evaluation (ACH50). He is a Handing Editor of *Transportation Research Record*, an Associate Editor of *Accident Analysis and Prevention*, and an Editorial Board Member of the *Journal of Transportation Safety and Security*.